An Exploration of the Otolithic Membrane's Structure and Elasticity

Asja Radja
Supervisor: Dr. Dolores Bozovic
University of California, Los Angeles Department of Physics and Astronomy Research for Undergraduates Experience 2011 Program

Abstract

High speed imaging was used to track pit boundary motion of the Otolithic Membrane of the bullfrog Sacculus. Preparations was isolated, mounted, and stimulated with physiological amplitudes and frequencies in solutions imitating the chemical composition of Endolymph *in vivo*. We observed the Otolithic Membrane coupling of hair bundles in directions both parallel and perpendicular to the axis of stimulation. Preliminary results also indicate a spatial variation of the membrane stiffness.

1. Introduction

1.1. Overview of transduction

The process of hearing involves the transduction of acoustic stimuli into neural impulses (Hudspeth, 2000). Sound waves from the outer world enter our ears as pressure waves and, through a molecular process within the inner ear, neural impulses are sent to the brain. The vestibular system processes ground-borne vibrations in an identical manner on a microscopic scale. Detection of linear and angular acceleration involves transduction of mechanical stimuli into electrical signals and uses the same biological structures as the hearing mechanism (Benser et al., 1993).

Transduction occurs in microscopic structures called hair bundles which are made of rows of 5-7µm long stereocilia of increasing height. They are linked together by non-elastic fibrous structures, tip links, which cause the stereocilia to be deflected in parallel when stimulated by a mechanical wave. These tip links are connected to mechanically-gated ion channels (Howard and Hudspeth, 1988; Markin and Hudspeth, 1955) when a sound wave deflects a hair bundle, the tension in the tip links causes these ion channels to open allowing an influx of ionic current (mostly potassium and some calcium) into the stereocilia. The surrounding fluid is called Endolymph and has a high concentration K^+ and a smaller concentration of Ca^{2+} and Na^{2+}. This influx of ions causes a depolarization in the stereocilia which then continues to propagate to the eight cranial nerve (Vollrath et al., 2007).

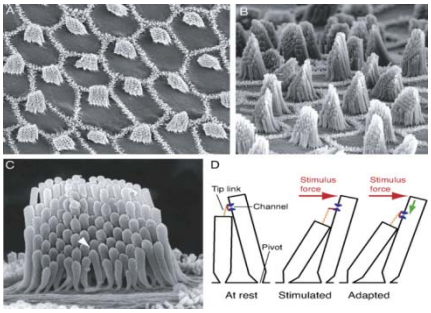

Figure 1: Hair Bundles and Mechanism (Hudspeth, 2008)

1.2. The Otolithic Membrane

In the inner ear organ, the Sacculus, of bull frogs (*Rana catesbiana*), around 1000 hair bundles are overlaid with a gelatinous, viscoelastic material called the Otolithic Membrane. This particular organ responds to linear accelerations and gravity and detects frequencies of 10-100 Hz. When an acoustic wave enters the inner ear, it stimulates the membrane and causes a shearing motion against the membrane underneath it called the macula (Kondrachuk, 2001). Because hair bundles are mechanically coupled to the Otolithic Membrane, the shearing of membranes with respect to each other causes the hair bundles to be deflected. The Otolithic Membrane couples the hair bundles to each other, phase-locking the responses of the many hair bundles underneath it (Strimbu et al., 2009).

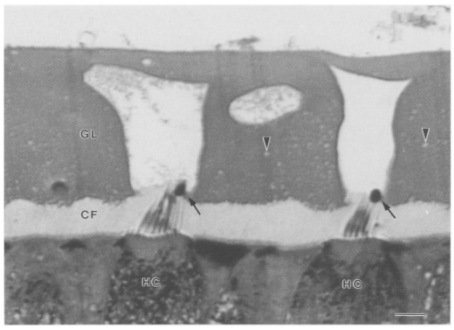

Figure 2: The Otolithic Membrane is the grey structure with two large holes in the top half of the image. Two hair bundles are depicted underneath it. The hair bundles are anchored to the bottom structure, the macula. (Kachar et al., 1990)

The Otolithic Membrane is a kidney bean-shaped membrane made of cross-linked filaments which make it a soft, gel-like, viscoelastic material. It is of relatively uniform thickness of 30µm and is 0.5mm across its long axis. Light Microscope images reveal that there are fluid-filled pits which surround the hair bundles and extend upwards near the top surface of the Otolithic Membrane (Kachar et al., 1990).

1.3. Motivation for studying the Otolithic Membrane

As coupling between hair cells has been proposed to enhance the sensitivity and frequency selectivity of the response, understanding the structure and properties of the Otolithic Membrane is important for understanding the performance of the whole organ. Extensive theory has been developed on the properties of viscoelastic materials and is applicable to the analysis of the Otolithic Membrane. In particular, the amplitude of localized displacement is expected to show a reciprocal decay with distance (Landau and Lifshitz, 1986). Alternatively, the Otolithic Membrane can be simplified to a model of a collection of springs – patches of membrane of a certain stiffness - in series with each other. If we define two spring constants, one for all springs between pit boundaries and the other for all those above pits, then we can examine whether there is anisotropy of elasticity in the membrane, with higher spring constants between pit boundaries than those above the pits. Additionally, most inner ear organs have specific orientations in relation to the body of the organism. Analysis of amplitude decay along different axes could therefore yield different relations.

Previous experiments done in the group examined preparations in which the Otolithic Membrane was left on top of the hair cells. It was found that a localized mechanical stimulus entrained bundle motion

across most of the epithelium (Strimb, 2009). Thus, we explore the properties of the Otolithic Membrane in isolation to better understand its contribution to the full system.

Although various inner ear organs detect different ranges of frequencies, they all display the same organization where hair bundles are held between two structures whose shearing motion causes the initiation of mechanotransduction. Hence, understanding the structure and properties of the Otolithic Membrane of the Sacculus may lead to insight into the general role of coupling in other inner ear organs (Benser et al., 1993).

2. Methods

2.1. Biological preparation

The Sacculus was isolated from the inner ear and the Otolithic Membrane was removed from the rest of the sample by enzymatic digestion. The membrane was fixed to a plastic mounting disk and placed in a two-compartment chamber (Martin et al., 2003). The Otolithic Membrane was fixed to the disk in two different ways to examine the effects of different boundary conditions. First, boundary conditions were fixed at the sides of the sample. A hole was punctured in a plastic disk, with an EM grid glued over it. A small opening was made in the grid, and the OM was attached to it by using a biological glue around its periphery. The second sample preparation was done by fixing the boundary conditions at the bottom of the OM. This was done by spreading 2.0µL of Concanavalin-A onto the surface of the plastic disk and, after allowing it to dry for roughly 45 minutes, placing the OM over the Concanavalin-A. Following this mounting process, the disks were placed in two compartment chambers in which both top and bottom compartments were filled with Endolymph to mimic *in vivo* solutions.

2.2. Stimulation, optical system, and tracking software

Stimulations were done using glass probes of infinite stiffness. They were pulled using a standard micropipette puller and the bent perpendicularly to create a hook-like end using a microforge. Probes were attached to a piezoelectric stimulator and lowered onto the Otolithic Membrane. Care was taken to lower the probe just enough to engage the membrane without damage. Sinusoidal displacements of various frequencies and amplitudes were sent to the piezoelectric crystal which stimulated the probe and Otolithic Membrane. Samples were viewed under an upright optical microscope (Olympus B51X) with a water-immersion objective. The pit walls were imaged at the focal plane which allowed for the greatest contrast. The sample's motion was then recorded with a high-speed Complementary Metal Oxide Semiconductor (CMOS) camera (Photon FASTCAM SA1.1) at a (1024 x 1024)-pixel resolution at 1000 frames per second. The software used to track the motion was developed in MatLab that fits a Gaussian curve to the intensity profile of the pit wall in each frame of the recordings. The software tracked the movement of pit walls in the x-axis only and extracted the traces of position versus time. These traces were then fit to sine waves in order to determine the amplitude and phase of the tracked motion. Further analysis and plots were done in Mathematica (Wolfram Research, Inc.).

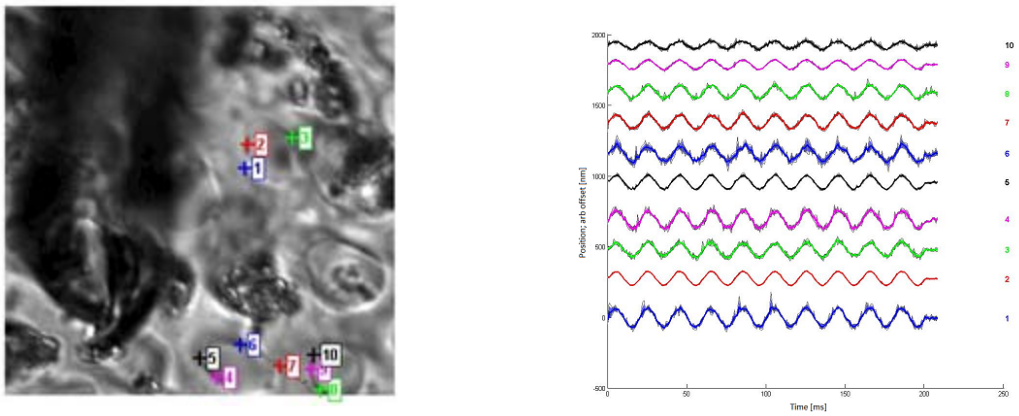

Figure 3: Example of screen with tracked points and complementary plots. Data taken from Prep 1 screen 1. The dark cylindrical object which comes into focus in the bottom left corner is the probe. The other dark crystal-like structures dispersed are calcium crystals common to some samples.

To test the hypotheses discussed in the Introduction, it was necessary to track broad areas of the epithelium, corresponding to several screens. Sequential recordings of 4-7 adjacent screens were performed with 10-20 pit boundaries contained in each screen. The fields of view were adjusted to contain some overlap between adjacent screens allowing for alignment of tiled images as shown in Figure 2 below. Because of the variation in the structure of the OM, not all pits could be in the focal plane during the tracking process; only pits that were clearly in focus were tracked. The OM was stimulated for each screen recording with the same signal sent to the piezoelectric driver. The recordings were triggered by the onset of the stimulus. Tracking of pit boundaries was always performed along the x-axis, the same axis as that of probe movement. During the tracking of pit boundary walls, a tolerance of 0.9 was maintained for the fitting of each intensity profile to a Gaussian distribution. An example of tracked points and resulting plots is shown below.

All protocols for animal care and dissection have been approved by the UCLA Chancellor's Animal Research Committee in accordance with state and federal guidelines.

3. Results

3.1. Parameters and Conditions of data sets

Four samples were mounted, stimulated, and recorded; all the relevant parameters are presented in table 1 below. All preparations were stimulated at 50Hz and an amplitude of 160nm. Preps 1 and 2 had boundary conditions imposed from the bottom as described in the methods section above, whereas preps 3 and 4 had boundary conditions imposed around the periphery of the OM. In prep 1, seven screens were recorded in the direction to the right; in prep 2, five screens were recorded in the same direction. In prep 3, four screens in the downward direction from the probe were tracked, to examine the effects of direction on the decay constants. In prep 4, we tracked four screens forming a square with the probe in the bottom left screen. Some ambiguity was present in establishing the orientation fot eh OM, whether pits faced towards or away from the camera during recordings. However, the long and short axes were readily discernible. It was noted that prep 1 was recorded along the long axis of the OM and prep 2 along the short axis. These variations allow us to preliminarily determine whether there is a dependence of the rate of amplitude decay on either axis of the OM.

	Prep 1	Prep 2	Prep 3	Prep 4
Boundary Conditions	Bottom	Bottom	Side	Side
Frequency (Hz)	50	50	50	50
Amplitude (mV)	400	400	400	400
Screens (#, direction)	7, across right	5, across right	4, down	4, square: across right and up

Table 1: Parameters and Conditions of Preparations

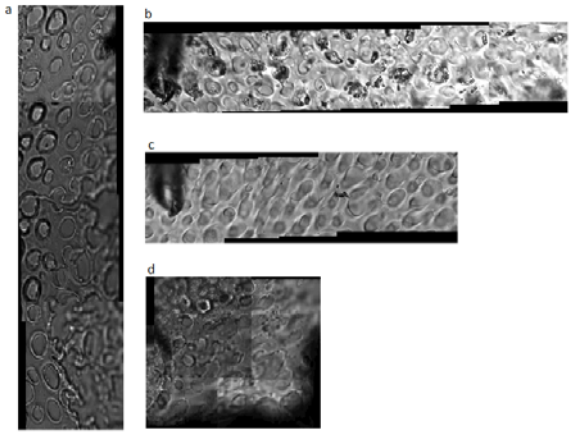

Figure 4: Tiled Images: a. Prep 3, b. Prep 1, c. Prep 2, d. Prep 4. The probe can be seen in all tilted images. In a, it is in the top right corner; and in b, c, and d, it is seen on the left. Glue can be seen on the left edge of figure a and around the periphery of figure d. Varying contrasts were used for different samples to examine which gave the best results.

3.2. Amplitude decay and phase lag across the otolithic membrane

Figure 5 summarizes the data for all four of the preparations. In the first two columns, the y axis denotes the amplitude of the induced pit boundary movement found by fitting a sine wave to the raw traces, and the x axis is the distance from the tracked point to the stimulus probe. The first column displays all of the data points with an overlaid exponential fit e-r and the second column with a reciprocal fit, -1/r, where r is the distance from the tracked point on the pit boundary wall to the stimulus probe. The third column displays the phase values of all tracked points as a function of the distance from the tracked point to the stimulus probe. The decay constants for both fits are given in table 2 below.

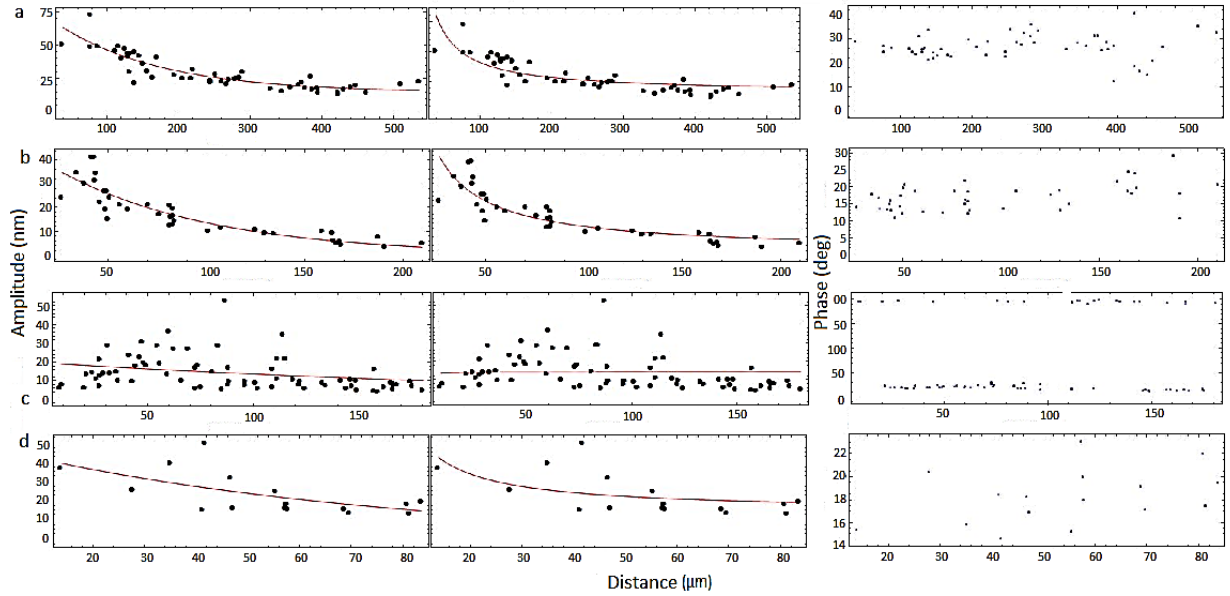

Figure 5: Column 1 is the exponential fit; Column 2 is the 1/r fit. a. Prep 1, b. Prep 2, c. Prep 3, d. Prep 4

	Exponential Fit Decay Constant (µm)	Reciprocal Fit Decay Constant (µm)
Prep 1	72	2500
Prep 2	78	1100
Prep 3	270	-6.9
Prep 4	74	390

Table2: Decay constants for above fits

3.3. Amplitude change between and above pit boundaries

As mentioned in the Introduction, the Otolithic Membrane can be viewed as a collection of springs in series with each other. We hypothesized that springs between pits would have a larger spring constant than springs above pits. This proposition was tested by tracking sides of adjacent pit boundaries. Three points were tracked: the first was the right edge of a particular pit, the second was the left edge of the immediate neighboring pit to the right, and the third was the right edge of the same pit. An example of this can be seen in Figure 4 below. Data from Prep 1 was used due for this analysis, due to the largest abundance of track-able neighboring pit walls. We then calculated the change in amplitude between and above boundaries per unit distance. A smaller change in amplitude per unit distance would represent a material with a larger elasticity constant. Table 3 below shows the values of the change in amplitude per unit distance observed for five different adjacent pits. The very last column is the quantity of the difference of values columns two and three divided by the average of these values. This value is used to determine the significance of the results of the data.

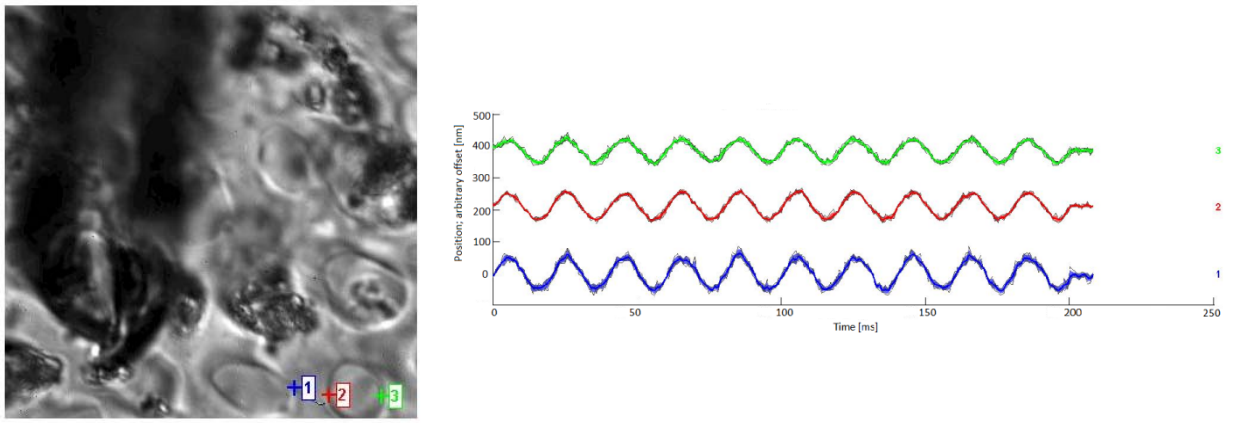

Figure 6: Tracking between and across pit boundary

Sample	Amplitude decay per unit distance between pits (mm)	Amplitude decay per unit distance above pits (mm)	Greater value	Significance
S1	0.0019	0.0090	Between	1.3
S2	0.0017	0.0022	Above	0.26
S3	0.00029	0.000066	Between	1.2
S4	0.0042	0.0025	Between	0.50
S5	0.0030	0.0018	Between	0.50
			Average	**0.76**
			Variance	**0.23**

Table3: Amplitude decay per unit distance between and across pit boundaries.

4. Discussion

The preliminary results of the above experiments imply that a significant amount of coupling of hair bundles is introduced by the OM. This is consistent with the notion that coupling improves the sensitivity and efficiency of the system. Both exponential and reciprocal dependences show fairly good fits to the data. Prep 1 indicates a decay constant of 72µm, which, given the average size of the pit boundaries and the average distance between adjacent pits, corresponds to the coupling of about seven hair cells. Prep 2 shows a decay constant of 78µm, corresponding to the coupling of about 8 hair cells.In the direction of probe stimulation, therefore, less than ten hair bundles are coupled. Exponential and reciprocal fits for prep 3, however, show very little amplitude decay in the direction perpendicular to probe stimulation. This preparation tracked movements in the x direction, and observed decay in four screens in the negative y direction. These preliminary results show a large decay constant of 270µm, corresponding to almost thirty hair cells. The decay constants in prep 4 were less conclusive due to the shorter distances, but were similar to those of preps 1 and 2.

There was very little phase variation in preps 1, 2, and 4. This was expected from the results of the previous study of the hair bundles coupled to the membrane. However, prep 3 showed unusual points exhibiting phase lags near 180 degrees, hence exact out-of-phase response. This couple be indicative of more complex modes of stimulus propagation, but the results are too preliminary to speculate.

As presented in the introduction, we explored spatial variation in stiffness by looking at the amplitude decay between and above pit boundaries. Our results indicated a surprising result, that the spring constant above the pits is predominately larger than that of the region between the pits. The spread of data is 30% of the average value. The values indicating that the amplitude decay is larger between pit boundaries (S1, S3-S5) exceeds the variance; whereas, the value (S2) - indicating a larger amplitude decay above pit boundaries - is fairly close to the variance value. Further statistics will be needed however to corroborate the results.

Finally, we compare these results to previous experiments done with the hair bundles coupled to the OM. In these experiments, a stimulation frequency of 50Hz and stimulation amplitude of 35nm were used. Although the amplitude is much smaller than used in these experiments, a decay constant of 237 µm was determined. Given that the decay constant was so much larger while the hair bundles were still attached in comparison to the results found in this experiment, this may be evidence that the active process in the hair bundles may be leading to an additional synchronization of their movement.

Several factors will examined in more detail in the future to improve upon these measurements. First, lowering of the probe onto the OM relies the subjective judgment of the experimenter, and could be made more automatic. Samples with side-imposed boundary conditions were however less sensitive to this problem. The effects of enzymatic digestion on the OM's elasticity and stiffness are also unknown. An exploration of this dependence could significantly change the results found in this preliminary investigation. In order to more closely imitate *in vivo* conditions, the OM should be studied without the enzymatic digestion.

5. Conclusions

The Otolithic Membrane was isolated, mounted, and stimulated with physiological amplitudes and frequencies. Movements of pit boundary walls within it were tracked in solutions imitating the chemical composition of Endolymph *in vivo*. Preliminary conclusions show that the Otolithic Membrane exhibits spatial constant of ~70μm, corresponding to the coupling of ~7 hair bundles; higher decay constants were seen in the direction perpendicular to the axis of stimulation. Preliminary results also showed that the amplitude decay between pit boundaries to be greater than that of regions above pit boundaries, indicating a spatial variation of the membrane stiffness.

Acknowledgements

I would first and foremost like to thank Dr. Dolores Bozovic for the opportunity, advice, support, direction, and ideas she provided me with. Without her none of this would have been possible. I would also like to thank Francoise Queval for her care, encouragements, and for the endless opportunities she offers. I would like to thank the Bozovic lab: Elliott Strimbu, Sebastian Meenderink, Lea Fredrickson-Hemsing, Albert Kao, Yuttana Roongthumskul, David Rowland, and Marcos Nunez. Time spent both in and out of the lab with you was time well spent. And finally, I would like to thank the National Science Foundation for their continual support and funding of this life-changing program.

References

Benser, M.E., Issa, N.P., Hudspeth, A.J., 1993. Hair-bundles stiffness dominates the elastic reactance to otolithic-membrane shear. Hear. Res. 68, 243-252.

Howard, J., Hudspeth, A.J., 1988. Compliance of the hair bundle associated with gating of mechanoelectrical transduction channels in the bullfrog's saccular hair cell. Neuron 1, 189-199.

Hudspeth, A.J., 2008. Making an effort to listen: Mechanical amplification in the ear. Neuron 1.

Hudspeth, A.J., 2000. Hearing. In: Kandel, E.R., Schwartz, J.H., Jessell, T.M. (Eds.), Princ. Neural Sci., McGraw-Hill, New York, 590 – 624.

Kachar, B., Parakkal, M., Fex, J., 1990. Structural basis for mechanical transduction in the frog vestibular sensory apparatus: I. The otolithic membrane. Hear. Res. 45, 179-190.

Kondrachuk, A.V., 2001. Models of otolithic membrane-hair bundle interaction. Hear. Res. 166, 96-112.

Landau, L.D., Lifshitz, E.M., Theory of Elasticity (3rd ed.), Pergamon Press, Oxford. 1986.

Markin, V.S., Hudspeth, A.J., 1995. Gating-spring models of mechanoelectrical transduction by hair cells of the internal ear. Annu. Rev. Biophys. Biomol. Struct. 24, 59-83.

Martin, P., Bozovic, D., Choe, Y., Hudspeth, A.J., 2003. Spontaneous oscillation by hair bundles of the bullfrog's Sacculus. J. Neurosci. 23, 4533-4548.

Strimbu, C.E., D. Ramunno-Johnson, D., Fredrickson, L., Arisaka, K., Bozovic, D. 2009. Correlated movement of hair bundles coupled to the otolithic membrane in the bullfrog Sacculus. Hear. Res. 256, 58-63.

Vollrath, M.A., Kwan, K.Y., Corey, D.P., 2007. The micromachinery of mechanotransduction in hair cells. Annu. Rev. Neurosci. 30, 339-365.